

# Cross-property relations for two-phase planar composites

H.F. Zhao <sup>a</sup>, G.K. Hu <sup>a,\*</sup>, T.J. Lu <sup>b,1</sup>

<sup>a</sup> *Department of Applied Mechanics, Beijing Institute of Technology, Beijing 100081, PR China*

<sup>b</sup> *Department of Engineering, University of Cambridge, Cambridge CB2 1PZ, UK*

Received 13 October 2004; received in revised form 24 February 2005; accepted 17 March 2005

## Abstract

The overall property of a composite material is dictated by parameters that characterize its microstructure. Theoretically, cross-links between different physical properties of the same material have been established by eliminating all or partially these microstructural parameters. Practically, such a correlation may be used to determine one property from another once the latter is measured or calculated: the success of this approach depends on whether the correlation is insensitive to the detailed material microstructure. In the present paper, cross-property relations for planar two-phase composites are examined using both analytical approaches and the digital-based finite element method. Both isotropic and transversely isotropic two-phase planar composites are studied. Focus is placed on studying how the microstructure (e.g., shape, size, distribution and volume fraction of inclusions) affects the correlation between two different overall properties of the composite. At a fixed volume fraction, questions on whether the correlation is one-to-one and whether it is sensitive to large material contrast (e.g., voids or rigid inclusions) or how the inclusions are distributed in the matrix will be answered.

© 2005 Elsevier B.V. All rights reserved.

*Keywords:* Cross-property relation; Two-phase planar composite; Finite element method; Effective properties

## 1. Introduction

The overall properties of a heterogeneous material depend intimately on its microstructure. These properties, including the elastic modulus, electrical/thermal/magnetic conductivity, dielectric coefficient and thermal expansion coefficient, are typically functions of the same microstructural parameters. One can eliminate all or partially these parameters and obtain the cross-link relations between two different classes of overall properties, e.g. elastic modulus and electrical conductivity. When

some macroscopic properties are difficult to measure, one can use the cross-relations to estimate these properties in term of the others. This idea has already been applied to practice: for example eddy current method is widely utilized for non-destructive evaluation of steel structural elements [1].

The idea of cross-property link was firstly proposed by Bristow [2] for a solid containing low density, randomly oriented microcracks: based on non-interaction approximations, cross-property relations between elastic modulus and conductivity were obtained. Levin [3] subsequently derived exact correlations between the effective bulk modulus and the thermal expansion coefficient of a fiber-reinforced composite. The cross-property bounds derived by Berryman and Milton [4] for two-phase composites provide improved bounds compared to the Hashin–Shtrikman (HS) bounds [5]. Gibiansky and Torquato [6] proposed to bound one effective property

\* Corresponding author. Fax: +86 10 68914780.

E-mail addresses: [hugeng@public.bta.net.cn](mailto:hugeng@public.bta.net.cn) (G.K. Hu), [tj21@cam.ac.uk](mailto:tj21@cam.ac.uk) (T.J. Lu).

<sup>1</sup> Also at: State Key Laboratory for Mechanical Strength and Structural Vibrations, Xi'an Jiaotong University, Xian, Shaanxi Province 710049, PR China.

from the bounds of others for any two-dimensional isotropic composite material. The correlations between the effective modulus and thermal conductivity of thermal barrier coatings (TBCs) made by physical vapor deposition have been established by Lu et al. [7] using the non-interaction approximation for a variety of anisotropic pore morphologies; a similar work can be found in [8] for plasma sprayed ceramic coatings. Kachanov et al. [9] and Sevostianov and Kachanov [10] derived, also in the framework of non-interaction approximation, explicit correlations between the effective modulus and electrical conductivity of two-phase composites and porous materials with anisotropic microstructures. Zhao et al. [11] performed numerical computations for different two-dimensional isotropic composites and porous materials: the numerically obtained cross-property relations compare favorably with the HS bounds. Experimental investigation of the cross-property link was addressed by Sevostianov et al. [12] for close-celled aluminum foams and by Sevostianov and Kachanov [13] for short fiber-reinforced thermoplastics.

The focus of this paper is on planar (two-dimensional) two-phase composites, with both numerical and analytical methods utilized to obtain the cross-property relations. The composites studied are either isotropic with random or periodic microstructures or transversely isotropic with aligned fibers or pores. The influence of microstructures and reinforced phase property on the cross-links is examined in detail. The paper is arranged as follows: cross-links derived with different analytical methods are presented in Section 2, numerical computations on a variety of microstructures are detailed in Section 3, and a comparison of the cross-property relations established by these two methods is given in Section 4.

## 2. Analytical cross-property relations

In this section, different micromechanical methods will be utilized to establish the cross-property relations between the effective modulus and thermal conductivity for planar composites. Both isotropic and transversely isotropic composites are considered. For simplicity, only the effective bulk modulus is discussed for isotropic materials. Here we assume a two-phase planar composite with  $(K_0, K_1)$ ,  $(\mu_0, \mu_1)$  and  $(\sigma_0, \sigma_1)$  representing separately the two-dimensional bulk moduli, shear moduli and thermal conductivities, where the subscripts (0, 1) refer to the matrix and inclusion phases, respectively. The volume fractions of the reinforced phase (or pores) and the matrix are denoted by  $c_0$  and  $c_1$  ( $c_0 + c_1 = 1$ ). For transversely isotropic composites, only the cross-links obtained with the HS bounds are given.

The micromechanical methods discussed in this paper have been well documented (see, e.g., [14]). Consequently, only the final results on cross-links are listed below.

### 2.1. Voigt and Reuss estimations

The Voigt upper bounds of the bulk modulus and thermal conductivity for a planar isotropic two-phase composite are

$$K_c = c_1 K_1 + (1 - c_1) K_0, \quad (1a)$$

$$\sigma_c = c_1 \sigma_1 + (1 - c_1) \sigma_0. \quad (1b)$$

In fact, Eq. (1) provides the upper limits for the effective bulk modulus and thermal conductivity, here we take these upper limits as the effective properties of the composite to establish the cross-link relation. The same assumption is made for Hashin–Shtrikman bound in the following section. From Eq. (1), one can eliminate the volume fraction of the inclusions,  $c_1$ , to obtain the cross-property relation, as

$$\bar{K}_c - 1 = \frac{(K - 1)}{(\sigma - 1)} (\bar{\sigma}_c - 1), \quad (2)$$

where  $\bar{K}_c = K_c/K_0$ ,  $\bar{\sigma}_c = \sigma_c/\sigma_0$ ,  $\sigma = \sigma_1/\sigma_0$  and  $K = K_1/K_0$ . Eq. (2) can be used to calculate  $K_c$  once  $\sigma_c$  is given, and vice versa. Note that this correlation is independent of the composite microstructure as well as the volume fraction of the inclusions. Similar observations apply to other analytical cross-links to be presented below.

The Reuss lower bounds for the bulk modulus and thermal conductivity are given by

$$K_c = \frac{K_1 K_0}{c_1 K_0 + (1 - c_1) K_1}, \quad (3a)$$

$$\sigma_c = \frac{\sigma_1 \sigma_0}{c_1 \sigma_0 + (1 - c_1) \sigma_1}. \quad (3b)$$

Eliminating  $c_1$  from Eq. (3) leads to

$$\left( \frac{1}{\bar{K}_c} - 1 \right) = \frac{1/K - 1}{1/\sigma - 1} \left( \frac{1}{\bar{\sigma}_c} - 1 \right). \quad (4)$$

### 2.2. Hashin–Shtrikman bound

More elaborated bounds for a two-phase isotropic composite than the Voigt and Reuss bounds are proposed by Hashin and Shtrikman [5]. In the two-dimensional case, the HS bounds for the bulk modulus and thermal conductivity are

$$\bar{K}_c = 1 + \frac{c_1}{\frac{1}{K-1} + \frac{(1-c_1)}{1+v}}, \quad (5a)$$

$$\bar{\sigma}_c = \frac{(1+c_1)\sigma + (1-c_1)}{(1-c_1)\sigma + (1+c_1)}. \quad (5b)$$

Eq. (5) gives a lower bound if  $K_0 < K_1$ ,  $\mu_0 < \mu_1$  and  $\sigma_0 < \sigma_1$ , and an upper bound if  $K_0 > K_1$ ,  $\mu_0 > \mu_1$  and  $\sigma_0 > \sigma_1$ . For spherical inclusions, Eq. (5) can also be obtained by the Mori–Tanaka method [15].

Combination of Eqs. (5a) and (5b) leads to the following cross-property relation [11]:

$$\frac{k(\bar{K}_c)}{k(K)} = \frac{\Sigma(\bar{\sigma}_c)}{\Sigma(\sigma)}, \quad (6)$$

where  $v = \mu_0/K_0$ ,  $k(x) = \frac{1}{x-1} + \frac{1}{v+1}$  and  $\Sigma(x) = \frac{x+1}{x-1}$ .

For a planar isotropic porous material, Eq. (6) reduces to

$$\frac{1}{\bar{K}_c} - 1 = \frac{1}{1 - v_0} \left( \frac{1}{\bar{\sigma}_c} - 1 \right), \quad (7)$$

where  $v_0$  is the Poisson ratio of the matrix material.

Consider now a two-dimensional composite with aligned elliptical inclusions, the HS bounds are provided by Willis [16], which can also be obtained by the Mori–Tanaka method if the ellipsoid characterized the distribution of inclusion is taken to be the same form as the inclusion [17,18]. If all the elliptical inclusions have the same form with aspect ratio  $\alpha$  and they are aligned with the axis  $x_1$ , Young's moduli of the composite along and perpendicular to the  $x_1$ -axis are

$$\bar{E}_{c1} = \frac{B - C}{R + S}, \quad (8a)$$

$$\bar{E}_{c2} = \frac{B - C}{W + Y}, \quad (8b)$$

where

$$B = -E^2[-3\alpha - c_1(2 + 2\alpha^2 + \alpha c_1) + 2\alpha(c_1 - 1)v_0 + \alpha(c_1 - 1)^2 v_0^2],$$

$$\bar{K}_c = \frac{K(1 - 2c_1 + v_0) - (1 - 2c_1 - v_0) - \sqrt{[K(1 - 2c_1 + v_0) - (1 - 2c_1 - v_0)]^2 - 4K(v_0^2 - 1)}}{2(v_0 - 1)}, \quad (11a)$$

$$\bar{\sigma}_c = \frac{1}{2} \left\{ 1 - 2c_1 - \sigma + 2c_1\sigma + \sqrt{4\sigma + (1 - 2c_1 - \sigma + 2c_1\sigma)^2} \right\}. \quad (11b)$$

$$C = 2(c_1 - 1)E\{1 + \alpha^2 + \alpha c_1 - \alpha[1 + (c_1 - 1)v_0]v_1\} + \alpha(c_1 - 1)^2(v_1^2 - 1),$$

$$R = \alpha(c_1 - 1)E^2(1 + v_0)[-3 + 2\alpha c_1(v_0 - 1) + v_0] + \alpha(c_1 - 1)(1 + 2\alpha c_1)(v_1^2 - 1),$$

$$S = 2E\{1 + \alpha^2 + 2\alpha c_1(1 - \alpha + \alpha c_1) - \alpha(c_1 - 1)[-1 + (1 + 2\alpha c_1)v_0]v_1\},$$

$$W = (c_1 - 1)E^2(1 + v_0)[\alpha(v_0 - 3) + 2c_1(v_0 - 1)] + (c_1 - 1)(\alpha + 2c_1)(v_1^2 - 1),$$

$$Y = 2E\{1 + \alpha^2 + 2c_1(\alpha + c_1 - 1) - (c_1 - 1) \times [(\alpha + 2c_1)v_0 - \alpha]v_1\}.$$

In the above relations, the normalized Young's moduli are defined as  $\bar{E}_{c1} = E_{c1}/E_0$ ,  $\bar{E}_{c2} = E_{c2}/E_0$  and  $E = E_1/E_0$ , and  $v_1$  is the Poisson ratio of the inclusion material.

The HS bounds for the effective conductivity of the same composite are

$$\bar{\sigma}_{c1} = \frac{1 - c_1 + c_1\sigma + \alpha\sigma}{1 + \alpha(c_1 + \sigma - c_1\sigma)}, \quad (9a)$$

$$\bar{\sigma}_{c2} = \frac{\alpha(1 - c_1 + c_1\sigma) + \sigma}{\alpha + c_1 + \sigma - c_1\sigma}. \quad (9b)$$

Although explicit cross-property relations can be derived in a direct way by eliminating  $c_1$  from Eqs. (8) and (9), the final expressions are complicated and hence will not be listed below. In the case of aligned elliptical pores, the cross-link relations simplify to

$$\bar{E}_{c1} = \frac{\bar{\sigma}_{c1}(1 + \alpha)}{1 + 2\alpha - \bar{\sigma}_{c1}\alpha}, \quad (10a)$$

$$\bar{E}_{c2} = \frac{\bar{\sigma}_{c2}(1 + \alpha)}{2 + \alpha - \bar{\sigma}_{c2}}, \quad (10b)$$

Note that for spherical voids ( $\alpha = 1$ ), Eq. (10) reduces to Eq. (7).

### 2.3. Self-consistent approximation

For a two-phase planar composite with spherical inclusions, its bulk modulus and thermal conductivity estimated by the self-consistent method are [19]

Eliminating  $c_1$  from Eqs. (11a) and (11b), the cross-property relation can be obtained. For porous materials, this leads to

$$\bar{K}_c - 1 = \frac{1}{1 - v_0} (\bar{\sigma}_c - 1). \quad (12)$$

### 2.4. Differential scheme

The expressions for the effective bulk modulus and thermal conductivity of a two-dimensional composite with spherical inclusions estimated by the differential scheme [20] are complicated. For a planar porous material with spherical pores, the results are

$$\bar{K}_c = \frac{3(1 - c_1)^3 v_0}{c_1[3 + c_1(c_1 - 3)](1 - 2v_0) + 3v_0}, \quad (13a)$$

$$\bar{\sigma}_c = (1 - c_1)^2. \quad (13b)$$

The cross-link relation can be established by eliminating  $c_1$  from (13).

### 3. Finite element simulations

The micromechanical methods outlined above are approximate, and they only apply for some specific microstructures. For example, the HS bounds are only attainable for hierarchical layered microstructures, and the self-consistent method is more suitable for polycrystalline microstructures without a specific matrix phase [21]. In order to examine whether the cross-property relations are sensitive to the microstructure of a material, we will in this section generate more complex and realistic microstructures, and compute the corresponding cross-property

relations using the finite element method (FEM). The comparison of the cross-property relations established by the two different methods will be given in Section 4.

Different microstructures are generated by the methods widely used in the computational physics community, including the random walk method and the cellular automata method [22]. Three classes of microstructures are analyzed, corresponding separately to the microstructures generated with spheres, random lattice and short fibers. For each class of the microstructure, different area fractions and physical properties of the inclusions (the white phase) will be examined. The images for the generated microstructures are shown in Figs. 1–3. For finite element simulations, each image is taken as the representative volume element (RVE) for the corresponding composite.

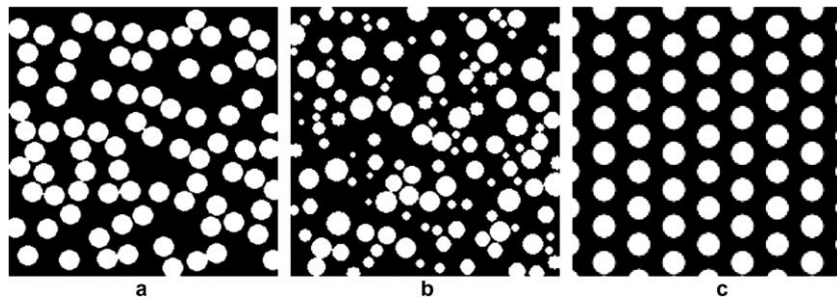


Fig. 1. Microstructures generated with impenetrable spheres: (a) mono-spheres,  $c_1 = 40\%$ ; (b) spheres with different sizes,  $c_1 = 35\%$ ; (c) spheres with an hexagonal distribution,  $c_1 = 32.3\%$ .

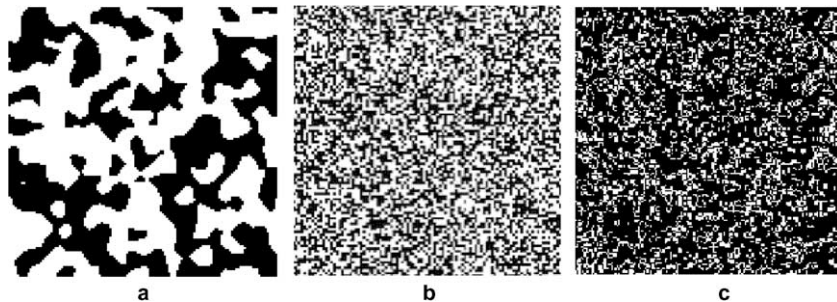


Fig. 2. Microstructures with random lattice generated with: (a) cellular automata simulation,  $c_1 = 45.7\%$ ; (b) checkerboard model,  $c_1 = 50\%$ ; (c) game of life simulation,  $c_1 = 5\%$ .

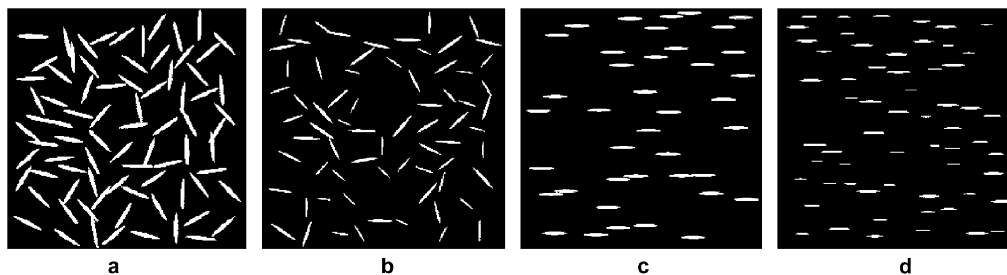


Fig. 3. Microstructure generated with short fibers (aspect ratio 1:10): (a) randomly oriented ellipses,  $c_1 = 14.5\%$ ; (b) randomly oriented ellipses with no uniform size,  $c_1 = 6.78\%$ ; (c) parallel ellipses along the  $x_1$ -axis,  $c_1 = 3.49\%$ ; (d) parallel ellipses along the  $x_1$ -axis with no uniform size,  $c_1 = 2.27\%$ .

Table 1  
Numerical accuracy for an image with different pixels

Image size	Bulk modulus	Shear modulus	Young's modulus	Poisson ratio	Thermal conductivity
32 × 32	1.6977 ± 0.0200	0.8448 ± 0.0089	2.2782 ± 0.0357	0.3351 ± 0.0073	2.7370 ± 0.0460
64 × 64	1.5766 ± 0.0119	0.7935 ± 0.0070	2.1134 ± 0.0252	0.3309 ± 0.0057	2.4628 ± 0.0236
128 × 128	1.5165 ± 0.0106	0.7626 ± 0.0061	2.0434 ± 0.0242	0.3308 ± 0.0059	2.3338 ± 0.0222
256 × 256	1.4963 ± 0.0149	0.7536 ± 0.0070	1.9985 ± 0.0196	0.3301 ± 0.0047	2.2747 ± 0.0199
320 × 320	1.4920 ± 0.0101	0.7523 ± 0.0059	1.9960 ± 0.0190	0.3298 ± 0.0040	2.2692 ± 0.0129

Numerical methods to evaluate the effective properties of composite materials are recently reviewed by Schmauder [23]. In the present paper, the digital-image-based finite element method developed by Garboczi [24] is utilized. This method is able to handle images as shown in Figs. 1–3 with an adequate resolution. In the computation, the digital images need to be saved in an ASCII format containing the values of square pixels at different gray scales.

With unit biaxial macroscopic strain imposed on the boundary of the RVE, local stresses and their spatial averages over the RVE are evaluated and subsequently used to calculate the effective modulus. For the effective thermal conductivity, a constant gradient of temperature is imposed at the boundary: the local heat flux is computed, and then averaged over the RVE.

To check the accuracy of the numerical method, the microstructure consisting of impenetrable mono-spheres with an area fraction  $c_1 = 44\%$  is chosen to be examined with different precisions (pixels). The following material constants are assumed:  $E_0 = 1$ ,  $E_1 = 10$ ,  $\sigma_0 = 1$ ,  $\sigma_1 = 10$ , and  $v_0 = v_1 = 1/3$ . The computed results are given in Table 1, where each value of the computed effective properties is the average of ten samples. It is found that the average values of the effective modulus, Poisson ratio and thermal conductivity stabilize for the digital image with more than  $64 \times 64$  pixels. In all subsequent computations, images with  $128 \times 128$  pixels are used.

The numerical results are further checked with the universal relations derived recently for planar composites and porous materials having arbitrary phase morphologies [25,26]. According to Hu and Weng [26], for any isotropic planar material containing arbitrarily shaped cracks or pores, the effective Young's modulus  $E_c$  and Poisson ratio  $v_c$  must satisfy the following universal relation:

$$(v_c - v_{c0})E_0/E_c = v_0, \quad (14)$$

where  $v_{c0}$  is the effective Poisson ratio of the same composite if the Poisson ratio of the matrix material is set to be zero. Similarly, for a transversely isotropic composite, one has [26]:

$$(v_{c12} - v_{c120})E_0/E_{c1} = v_0, \quad (15)$$

where the  $x_2$ -axis is taken to be perpendicular to the crack surface,  $v_{c120}$  is the effective in-plane Poisson ratio of the composite if the Poisson ratio of the matrix mate-

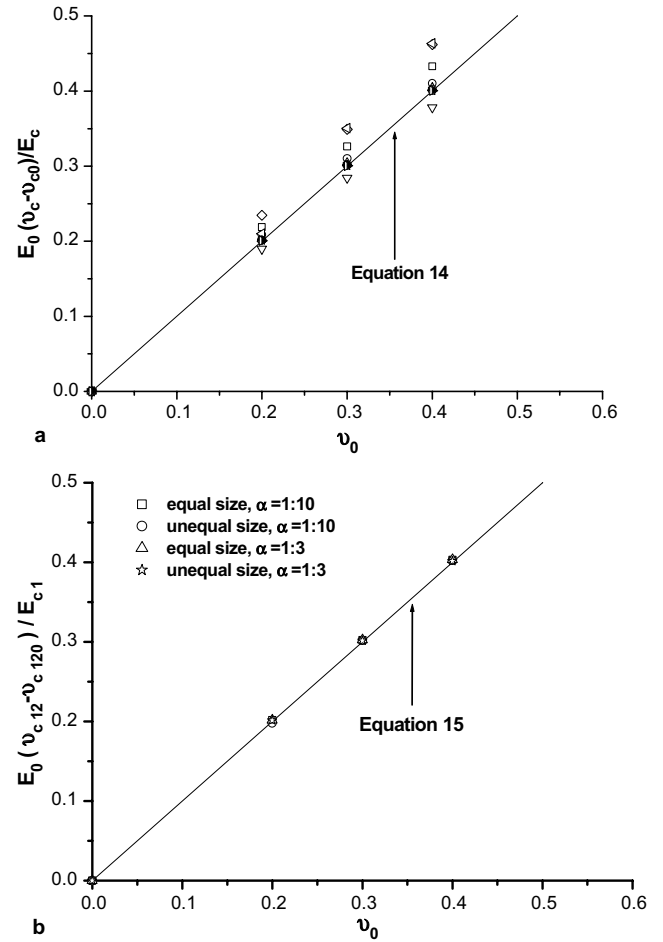


Fig. 4. Comparison between numerical results and universal relation: (a) isotropic composites; (b) transversely isotropic composites with aligned pores. Symbols: FEM calculation; solid line: universal relation.

rial is zero, and  $(E_{c1}, v_{c12})$  are the effective Young's modulus and effective Poisson ratio of the composite.

By setting the inclusion phase to be void, the effective moduli and Poisson ratio of the microstructures shown in Figs. 1–3 can be calculated accordingly. Fig. 4(a) shows the results for isotropic microstructures, and the comparison with Eq. (14) is also provided. For porous materials having aligned elliptical pores (Fig. 3(c) and (d)), comparison is given in Fig. 4(b). Overall, the numerical results agree well with the analytical universal relations for both isotropic and transversely isotropic composites.

### 4. Comparison and discussion

Cross-property relations established by both analytical and numerical methods are compared below. The results are grouped into two classes: one (Fig. 5) for isotropic composites and the other (Fig. 6) for transversely isotropic composites.

#### 4.1. Isotropic composites

For isotropic composites, the following material contrasts are examined:  $E_0:E_1 = \sigma_0:\sigma_1 = 1:0$  (Fig. 5a), 1:10 (Fig. 5(b)) and 1:10000 (Fig. 5(c)), corresponding respectively to a voided material, an inclusion-matrix material and a rigid inclusion material. In all computations,  $\nu_0 = \nu_1 = 1/5$  is assumed. It is found that for isotropic two-phase composites with modest contrast (Fig. 5(b); also see more in detail in Fig. 6), the cross-property relations are insensitive to the detailed microstructures, and can be well predicted by the analytical methods (e.g., the

HS bounds). There exists a one-to-one correlation between the effective bulk modulus and the effective thermal conductivity, irrespective of the underlying microstructure. For such composites, the established cross-links should be useful in engineering applications.

For isotropic composites with distributed voids or rigid inclusions, however, the cross-property relations predicted by both analytical and numerical methods exhibit pronounced scattering (see Fig. 5(a) and (c)). One must then be cautious when using these cross-property links in practice.

Fig. 6 presents more results for isotropic composites having varying phase contrasts:  $E_1:E_0 = \sigma_1:\sigma_0 = 1:0, 1:10, 1:400, 1:1000$ . Again,  $\nu_0 = \nu_1 = 1/5$  is assumed. The microstructures analyzed include those shown in Figs. 1(a), 2(b) and 3(a), and the numerical results are compared with those derived from the HS bound (Eq. 6). Fig. 6 clearly shows that for an isotropic composite with modest contrast, the cross-property relations are insensitive to its microstructure and can be well

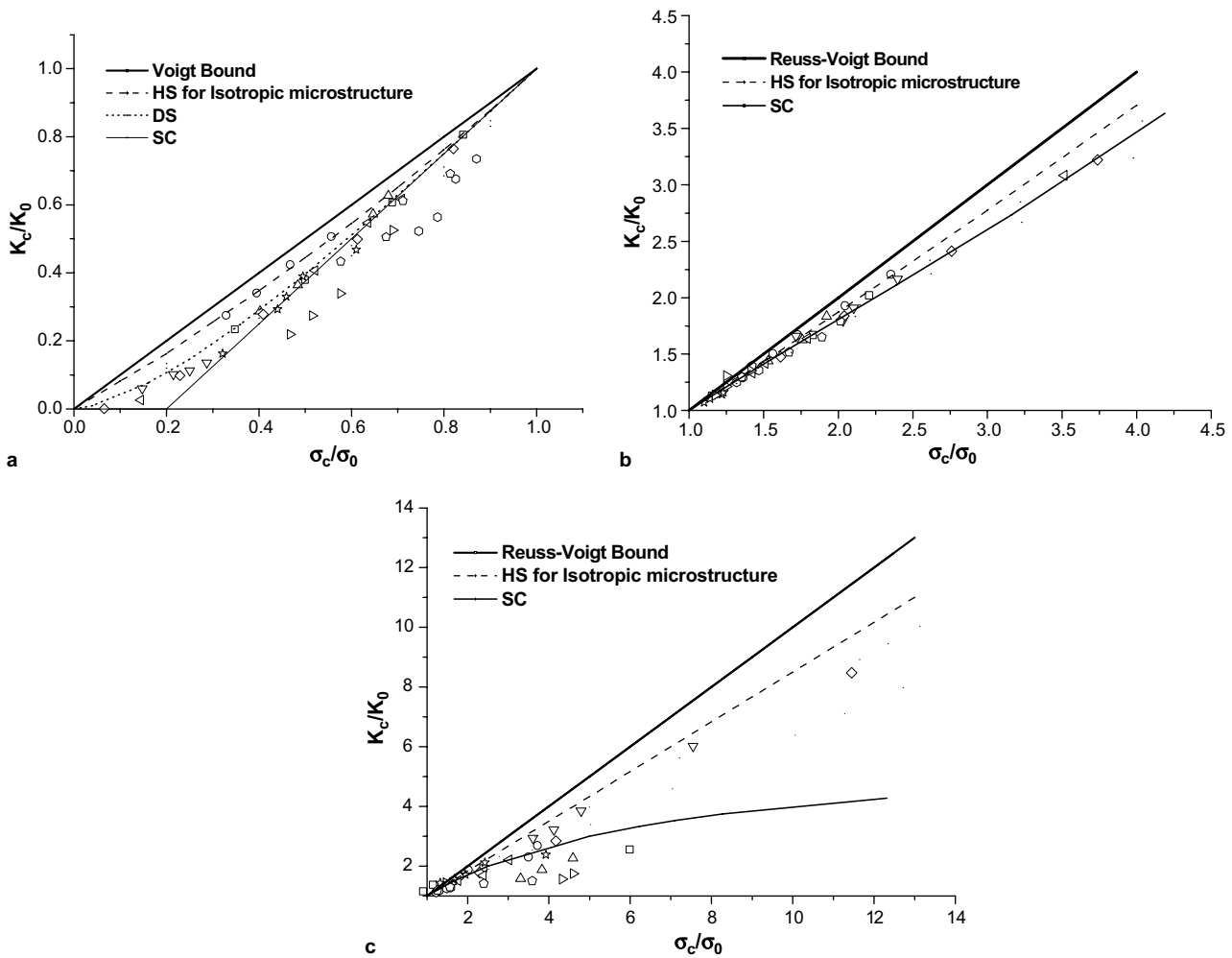


Fig. 5. Cross-property relations for isotropic composites: (a) porous materials; (b) inclusion-matrix materials with  $E_0:E_1 = 1:10$ ; (c) rigid inclusion with  $E_0:E_1 = 1:10000$ . Symbols: FEM calculation; line: analytical prediction.

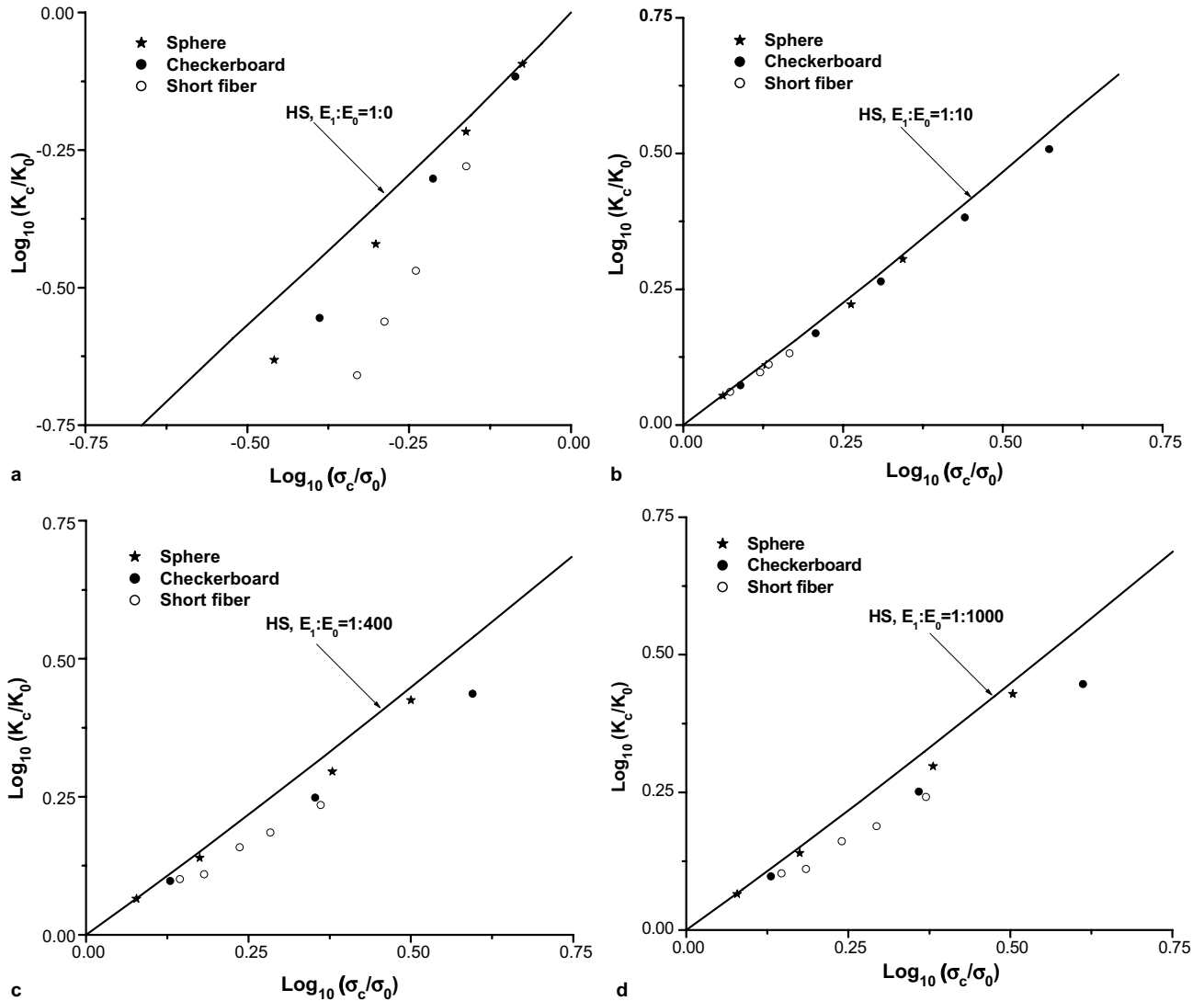


Fig. 6. Cross-property relations for isotropic composites with varying phase contrast: (a)  $E_0:E_1 = 1:0$ ; (b)  $E_0:E_1 = 1:10$ ; (c)  $E_0:E_1 = 1:400$ ; (d)  $E_0:E_1 = 1:1000$ . Symbols: FEM calculation; solid line: HS bounds.

predicted by either the HS lower or upper bounds (depending on the phase contrast). With high phase contrast, however, the scatter is more pronounced, especially for composites with high volume concentrations of inclusions. These results are expected: for a voided or rigid inclusion composite, its effective properties may vary dramatically near the percolation threshold.

#### 4.2. Transversely isotropic composites

Composites with aligned fibers or pores as a whole are transversely isotropic (Fig. 3(c) and (d)). For such composites, the cross-property relations established by the HS bounds and the numerical method agree excellently with each other, as shown in Fig. 7(a) and (b). It is believed that, in this situation, the microstructures are relatively regular and hence there is good

one-to-one correspondence between effective modulus and effective conductivity.

## 5. Conclusions

Cross-property relations for planar two-phase composites with varying microstructures are established using both analytical and numerical methods. For transversely isotropic composites having aligned elliptical fibers (or pores) with different volume fractions and aspect ratios, there is good correlation between analytical and numerical predictions, and the correspondence between two different physical properties is one-to-one: the results are insensitive to how the inclusions are aligned in the matrix. It is therefore possible to determine one property (e.g., thermal conductivity) from

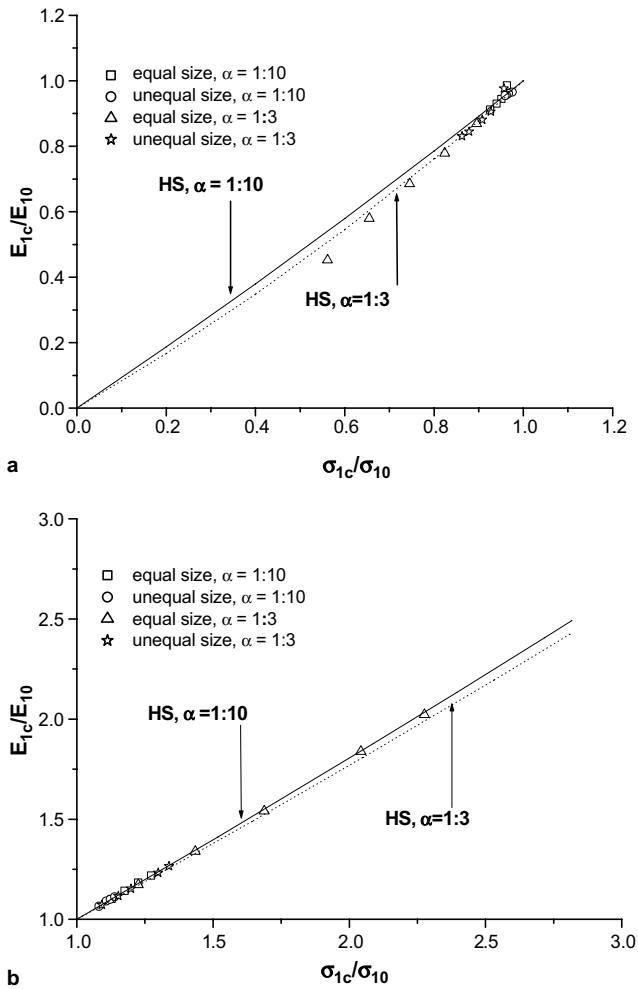


Fig. 7. Cross-property relations for transversely isotropic composites: (a) porous materials with  $E_0:E_1 = 1:0$ ; (b) inclusion-matrix materials with  $E_0:E_1 = 1:10$ . Symbols: FEM calculation; line: analytical prediction.

another (e.g., Young's modulus) once the latter is measured or calculated.

For isotropic two-phase composites, the above conclusion still holds if the contrast between the two phases is not large. For composites with large material contrast (e.g., voids or rigid inclusions), the cross-links are sensitive to how the inclusions are distributed in the matrix. The situation is particularly acute when the volume fraction of the inclusions becomes large. The cross-property correlations must then be used with caution in practice. The same idea can also be applied for a three-dimen-

sional composite to establish the cross-link relations, this will be our future work.

## Acknowledgment

This work was supported by the National Natural Science Foundation of China through grant 10325210.

## References

- [1] P. McIntire, Non-Destructive Testing Handbook, 2nd ed., Electromagnetic Testing, vol. 4, American Society for Nondestructive Testing, London, 1986.
- [2] J.R. Bristow, British J. Appl. Phys. 11 (1960) 81–85.
- [3] V.M. Levin, Mech. Solids 2 (1967) 58–61.
- [4] J.G. Berryman, G.W. Milton, J. Phys. D: Appl. Phys. 21 (1988) 87–94.
- [5] Z. Hashin, S. Shtrikman, J. Mech. Phys. Solids 11 (1963) 127–140.
- [6] L.V. Gibiansky, S. Torquato, Proc. R. Soc. Lond. A 452 (1996) 253–283.
- [7] T.J. Lu, C.G. Levi, H.N.G. Wadley, A.G. Evans, J. Am. Ceram. Soc. 84 (2001) 2937–2946.
- [8] I. Sevostianov, M. Kachanov, Mater. Sci. Eng. A 297 (2001) 235–343.
- [9] M. Kachanov, I. Sevostianov, B. Shafiro, J. Mech. Phys. Solids 49 (2001) 1–25.
- [10] I. Sevostianov, M. Kachanov, J. Mech. Phys. Solids 50 (2002) 253–282.
- [11] H.F. Zhao, G.K. Hu, T.J. Lu, Int. J. Fract. 126 (2004) L11–L18.
- [12] I. Sevostianov, J. Kovaik, F. Simanik, Int. J. Fract. 144 (2002) L23–L28.
- [13] I. Sevostianov, M. Kachanov, Mater. Sci. Eng. A 360 (2003) 339–344.
- [14] S. Nemat-Nasser, M. Hori, Micromechanics: Overall Properties of Heterogeneous Materials, Elsevier, North-Holland, 1993.
- [15] T. Mori, K. Tanaka, Acta Metall. Mater. 21 (1973) 571–574.
- [16] J.R. Willis, J. Mech. Phys. Solids 25 (1977) 185–202.
- [17] G.J. Weng, Int. J. Eng. Sci. 30 (1992) 83–92.
- [18] G.K. Hu, G.J. Weng, Mech. Mater. 32 (2000) 495–503.
- [19] S. Torquato, Random Heterogeneous Materials: Microstructure and Macroscopic Properties, Springer-Verlag, New York, 2002.
- [20] A.N. Norris, Mechanics of Materials 4 (1985) 1–16.
- [21] G.A. Milton, The Theory of Composite, Cambridge University Press, Cambridge, 2002.
- [22] D.H. Rothman, S. Zaleski, Lattice-Gas Cellular Automata Simple Models of Complex Hydrodynamics, Cambridge University Press, Cambridge, 1997.
- [23] S. Schmauder, Annu. Rev. Mater. Res. 32 (2002) 437–465.
- [24] E.J. Garboczi, Finite element and finite difference programs for computing the linear electric and elastic properties of digital images of random materials, NIST Internal Report 6269, 1998.
- [25] A. Cherkaev, K. Lurie, G.W. Milton, Proc. R. Soc. Lond. A 438 (1992) 519–529.
- [26] G.K. Hu, G.J. Weng, Proc. R. Soc. Lond. A 457 (2001) 1675–1684.